CHAPTER 4

Fabrication and Characterization of FTO/ZnO Seed Layer/ ZnO Nanorods/$CH_3NH_3PbI_3$/PTAA/Au Solar Cells with Different Seed Layers*

Contents

4.1 Introduction 86

4.2 Experimental Details 87

4.2.1 Solution Preparation for Seed Layer 87

4.2.2 Growth of ZnO Nanorods 89

4.2.3 Solar Cell Fabrication 91

4.3 Results and Discussion 92

4.3.1 Thin Film Surface Characterization 93

4.3.2 Optical Characterization 95

4.3.3 Electrical Characterization 98

4.4 Conclusion 102

CHAPTER 4

Fabrication and Characterization of FTO/ZnO Seed Layer/ ZnO Nanorods/$CH_3NH_3PbI_3$/PTAA/Au Solar Cells with Different Seed Layers

4.1 Introduction

The effects of thickness and surface morphology of hydrothermally grown TNRs based ETL on the performance of FTO/TNRs/$CH_3NH_3PbI_3$/PTAA (or Spiro-OMeTAD)/Pd perovskite solar cells (PSCs) have been investigated in Chapter-2 and Chapter-3 respectively. It is discussed in Chapter-1 that, like the TiO_2 nanorods (TNRs), ZnO nanorods (ZNRs) can also be used for the ETL in the solar cells [154]. In view of the above, we will now explore the hydrothermally grown ZnO nanorods (ZNRs) for the ETL in the PSCs in this chapter. The ZnO seed layer on the FTO substrate deposited by various methods can be used for the growth of ZNRs by the hydrothermal method. Various methods such as spray pyrolysis, electrochemical deposition, CVD, spin coating, sol-gel, dipping method, etc., are used for the seed layer deposition on the FTO substrates [155]-[158]. The deposition method of the seed layer plays a crucial role in determining the properties of the ZNRs grown by hydrothermal methods [90]. In this chapter, four different types of ZnO seed layers of drop-casted ZnO film, spin-coated colloidal ZnO nanoparticles (NPs) film, spin-coated colloidal ZnO quantum dots (QDs) film, and hydrothermally grown ZnO NRs film were deposited on four FTO substrates. The seed layer coated FTO substrates were then processed for growing ZnO NRs (ZNRs) based ETL by the hydrothermal method. Then spin-coated $CH_3NH_3PbI_3$ hybrid perovskite active layer and PTAA based HTL layers and thermally evaporated Au film

for contact electrode were successively deposited for fabricating four different PSC devices. The effects of coverage density, surface morphology, and orientation of the four different types ZNRs based ETLs on the performance parameters of FTO/TNRs/$CH_3NH_3PbI_3$/PTAA/Au structure-based PSCs have been investigated in this chapter. The content of the present chapter is outlined as follows:

Section 4.2 describes the details of the deposition process of ZnO seed layers, ZNRs, and the fabrication of PSCs. The measurement results for different seed layers and subsequent discussion are presented in Section 4.3. Finally, Section 4.4 summarizes the major finding and observations of this chapter.

4.2 Experimental Details

In this section, deposition of different seed layers, hydrothermal growth of ZNRs, and fabrication steps for different types of ZNRs based PSCs are presented.

4.2.1 Solution Preparation for Seed Layer

The FTO coated substrates (15 × 15 mm^2) were first cleaned using soap solution and rinsed in deionized (DI) water. Subsequently, the substrates were cleaned with acetone, 2-propanol, and then dried at 90°C for 10 minutes. Four different types of seed layer samples were prepared for the growth of ZNRs using ZnO drop-cast, ZnO nanoparticles (NPs), ZnO quantum dots (QDs), and solvothermal (ZnO NRs itself). The solution for the first sample (ZnO drop-cast) was made using 25 mM of zinc acetate dihydrate and 50 mM of sodium hydroxide (NaOH) in ethanol [159]. The sodium hydroxide solution was added dropwise to the zinc acetate dihydrate solution under vigorous stirring at 65^0C for 2 hours. The prepared solution was washed with ethanol several times after completing the reaction. The “ZnO NPs” sample was synthesized using 0.1 M solution of zinc nitrate ($Zn(NO_3)_2.6H_2O$) and 0.2 M solution of potassium

hydroxide (KOH) in DI water [160]. The KOH solution was added slowly into the zinc nitrate solution and kept under vigorous stirring continuously for 1 hrs. The prepared solution has an appearance of milky white in color. Finally, the solution was centrifuged at 5000 rpm for 5 min and was then washed with ethanol. Further, the prepared NPs are dried, and 10 mg of NPs are dissolved in 1 ml of chloroform.

"ZnO QDs" was prepared by mixing zinc acetate dihydrate (100 mM) in 2-methoxy ethanol (coordinating ligand) and constantly stirred on a hot plate at a temperature of 60°C in a nitrogen environment. An equimolar concentration of monoethanolamine (MEA) was added drop-by-drop in the solution at a constant temperature of 60^0C with continuously stirring [161].

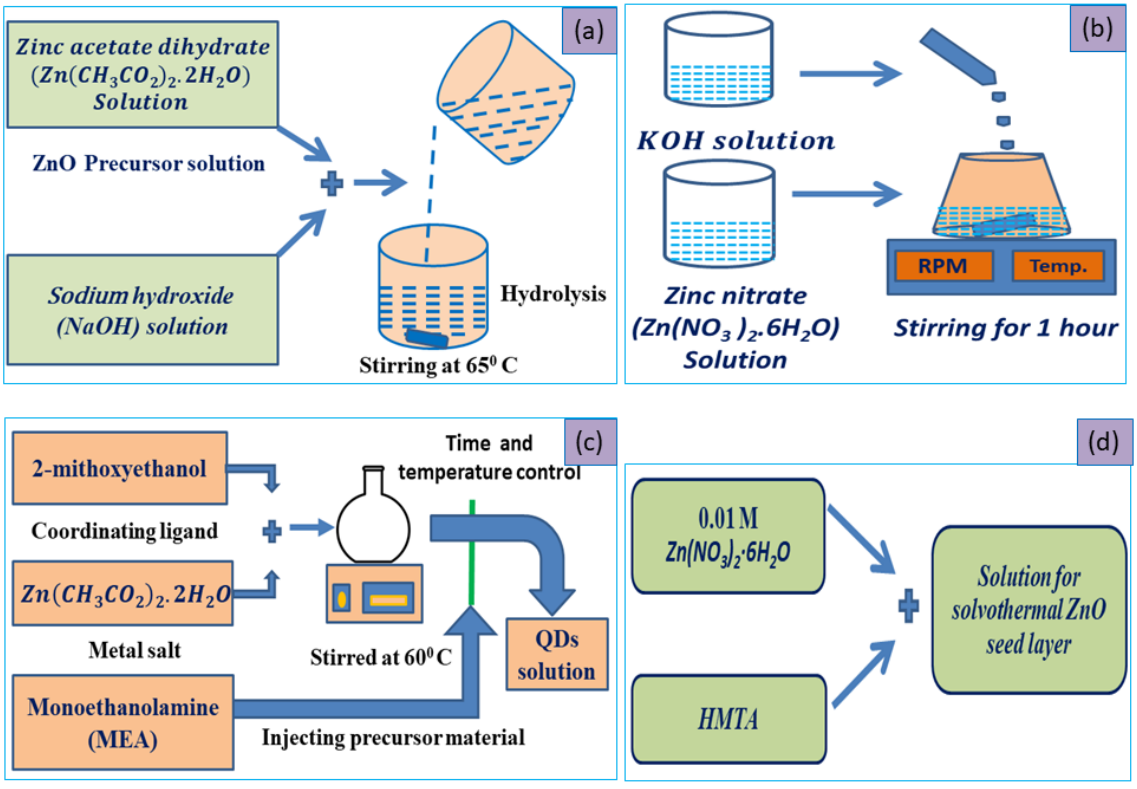

Figure 4.1: Graphical view of the preparation process of the solutions for the seed layers (a) ZnO drop-cast (b) ZnO NPs (c) ZnO QDs (d) Solvothermal ZnO NRs.

By controlling the reaction time, a uniform particle size of ZnO QD is obtained in

the order of Bohr's radius (~2.34 nm for ZnO). After that solution was filtered out by using a PVDF filter (0.22 μm) to remove unreactive particles. The last sample, "ZnO solvothermal," was prepared by using a mixture of 0.01 M concentration of zinc nitrate hexahydrate ($Zn(NO_3)_2 \cdot 6H_2O$) and HMTA in DI water. The ZnO seed layer solution preparation is graphically demonstrated in Figure 4.1.

4.2.2 Growth of ZnO Nanorods

There are several methods reported for the fabrication of the ZNRs. In the present work, the hydrothermal synthesis route was used for the fabrication of nanorods. A seed layer of different precursor solutions was deposited with the help of drop-cast, spin coating, and solvothermal methods. 40 μl precursor solution of the first sample was deposited using drop-cast technique onto cleaned FTO substrate, and the substrate was dried on a hot plate. This method (step) was repeated several times and annealed at 350^0C for 1 hour in ambient condition. The seed layer in sample 2 (NP) and 3 (QDs) were deposited via spin coating (SPM-150LC, GmbH) technique at 3000 rpm for 30 sec and heated on the hot plate at 100°C for 10 minutes. This process was repeated 3 times for the conformal deposition of the seed layer. The seed layer in sample 4 was deposited by hydrothermal process. FTO coated substrate (FTO side kept facedown) was immersed vertically in prepared solution in Teflon lined stainless steel autoclave for 1 hour at 90^0C for growth of ZnO seed layer. After the set time, the autoclave was kept outside the furnace and cooled slowly till room temperature. The sample was taken out from the autoclave and washed with running DI water several times, and dried with N_2 gas flow. The sample was rinsed in DI water and annealed at 150^0C for 1 hour to form a ZnO compact layer, which acts as a seed layer. Finally, all the seed layer coated substrate was annealed at 350°C. The deposition process of different seed layers is

illustrated in Figure 4.2.

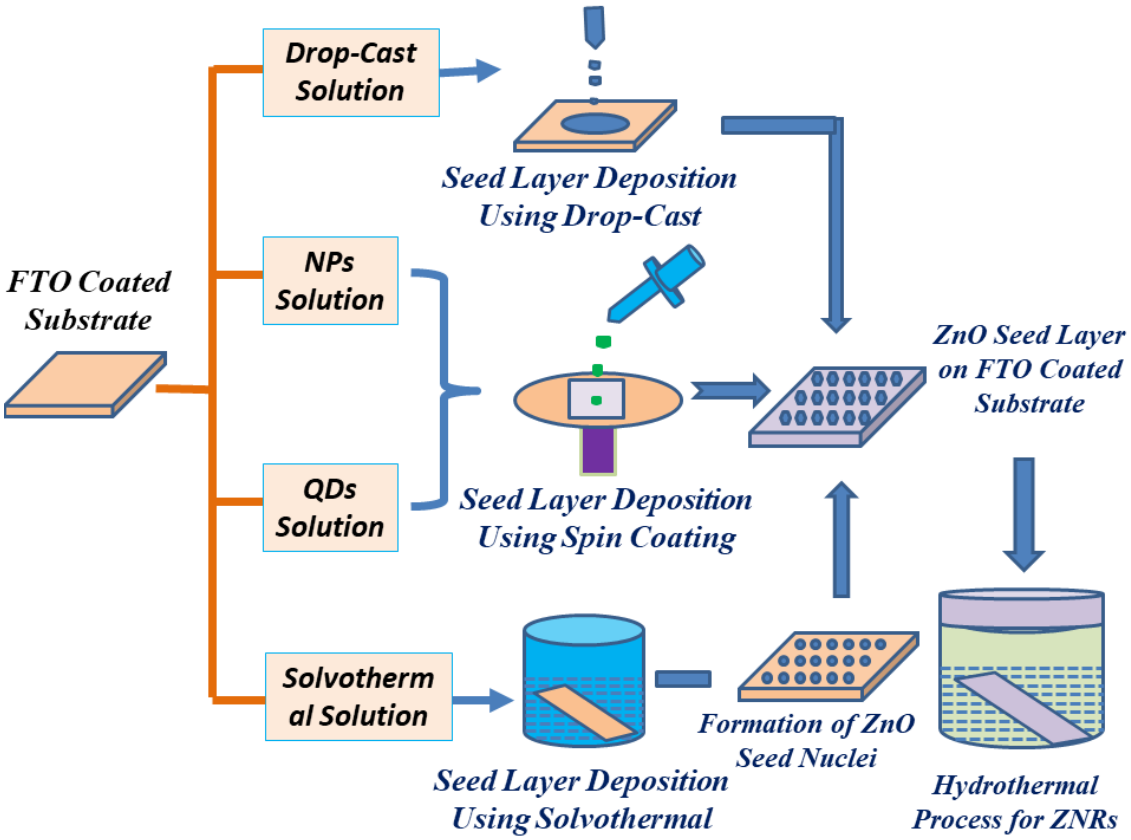

Figure 4.2: Seed layer deposition process using drop-cast, spin coating, and solvothermal. Growth of nanorods in the last step using the solvothermal process.

The seed layer coated FTO substrates were placed in the autoclave for the hydrothermal process as discussed for the seed layer of sample 4 and shown in Figure 4.2. The ZnO nanorod (ZNRs) on every sample was grown using an equimolar 50 mM solution of zinc nitrate hexahydrate ($Zn(NO_3)_2 \cdot 6H_2O$) and hexamethylenetetramine (hexamine) in DI water at 65^0C for 2 hours. Zinc nitrate and hexamethylenetetramine were used as the source of Zn^+ and OH^-, respectively in the hydrothermal process. No precipitate occurred when hexamine was mix in solution. By increasing in temperature, hexamine was converted into $Zn(OH)_2$ by decomposition. Further, the ZnO nuclei were created on the sample and continuously increased with time. The nuclei grew up, and

the thin film of ZnO formed on the sample. The possible reaction mechanism for ZNRs growth is given as [162]:

$$(CH_2)_6N_4 + 6H_2O == 6HCHO + NH_3 \quad (4.1)$$

$$NH_3 + H_2O == NH_4^+ + OH^- \quad (4.2)$$

$$2OH + Zn^{2+} == Zn(OH)_2 \quad (4.3)$$

$$Zn(OH)_2 == ZnO_{(s)} + H_2O \quad (4.4)$$

4.2.3 Solar Cell Fabrication

A hybrid perovskite layer was coated on the ZNRs via a two-stage spin coating method. The separate precursor solution of methylammonium iodide (CH_3NH_3I (~ 10 mg)) and lead iodide (PbI_2 (~ 462 mg)) was prepared in 1 ml of 2-propanol and N, N-dimethyl formamide (DMF) solvent. A solution of PbI_2 was heated at 90°C and continuously stirred at 300 rpm for 1 hour on the hot plate. 50 µl of this solution was then spin-coated at 3000 rpm for 30 seconds and heated at 70°C for 10 minutes on the hot plate. After that, the CH_3NH_3I solution was spin-coated at 3000 rpm as the second precursor. Toluene was used as an anti-solvent on top of perovskite thin-film during spin coating, which improves the surface morphology as well as conductivity by removing the voids and residues from methylammonium and halide ions [41]. The film was then heated at 100°C for 30 minutes to improve the crystallinity of the film. A thin layer (~100 nm) of PTAA was spin-coated at 2000 rpm for 30 s for the proper charge separation from the active layer (i.e., perovskite layer).

Finally, a thin layer (~80 nm) of gold (Au) was deposited on PTAA, which acts as a top electrode by using a thermal evaporation unit (FL400, HHV). The detailed

fabrication step is depicted in Figure 4.3. A comparative study was done to investigate the effect of different types of the seed layer on the PSCs' parameter. The four different types of PSCs have been fabricated with a different seed layer and named as follows:

PSC A:-Au/PTAA/$CH_3NH_3PbI_3$/ZNRs/ZnO Drop-cast seed layer/FTO

PSC B:-Au/PTAA/$CH_3NH_3PbI_3$/ZNRs/ZnO NPs seed layer/FTO

PSC C:-Au/PTAA/$CH_3NH_3PbI_3$/ZNRs/ZnO QDs seed layer/FTO

PSC D:-Au/PTAA/$CH_3NH_3PbI_3$/ZNRs/ZnO NR seed layer/FTO

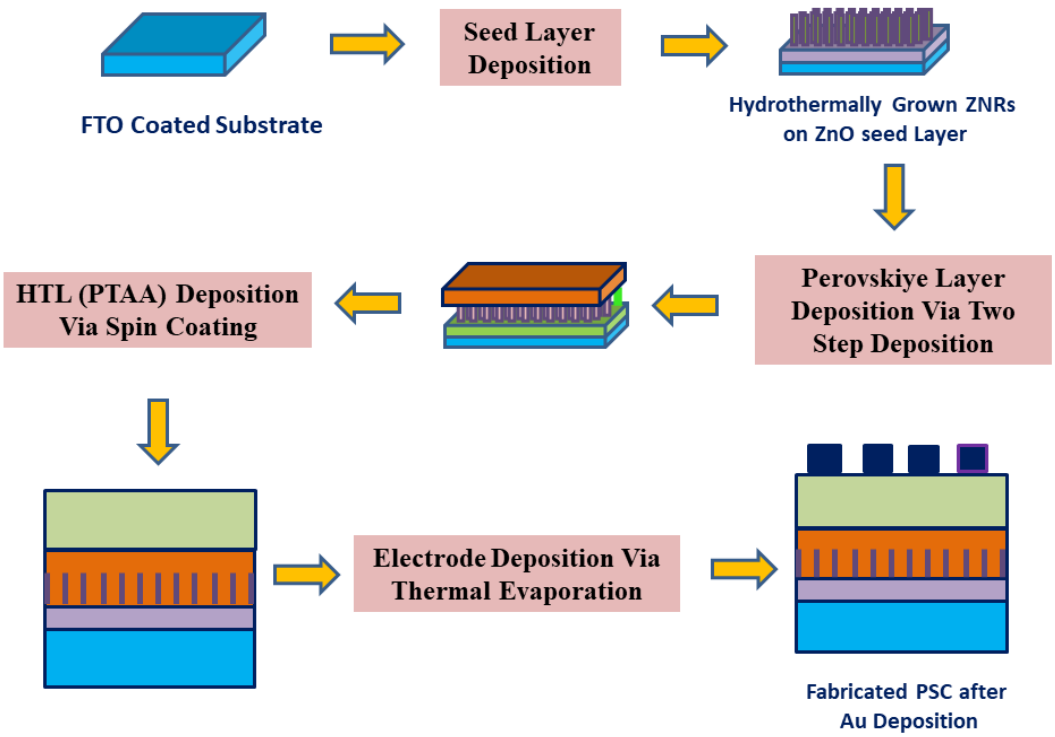

Figure 4.3: Fabrication flow diagram for the perovskite solar cell.

4.3 Results and Discussion

This section presents the optical and electrical characterizations of PSCs fabricated with different ZnO seed layers.

4.3.1 Thin Film Surface Characteristics

The scanning images of the top view of ZNRs grown on on different seed layer of ZnO deposited using drop-cast, spin coating, and solvothermal is shown in Figure 4.4. A significant morphological difference is observed. The nanorods which are grown on the first sample (ZnO seed layer by drop cast) are not well aligned and randomly distributed on the substrate. The growth is not perpendicular to the c-axis, even though growth is observed in all directions. It happened since the seed layer is not uniformly distributed throughout the substrate. The growth of ZNRs is uniform, well-distributed, and aligned for the ZnO QDs based seed layer. The nanorods' growth is in all directions and also perpendicular to the c-axis. It is possible because of the uniform growth of the seed layer. The size distribution and alignment of ZNRs are highly influenced by the particle size and the surface roughness of the seed layer. The particle of the seed layer acts as a nucleation center for the growth of ZNRs. The ZnO seed layer deposited from NPs solution has a larger particle size compared to ZnO QDs coated sample. It is shown in Figure 4.4 (b) and (c) that the diameter of ZNRs is more in the ZnO NPs based seed layer. It is observed from the SEM image that the surface to volume ratio is more in NPs and QDs seed layer based ZNRs compared to the other two samples, and it's also confirmed from the TEM image shown in the inset of Figure 4.4 (b) and (c). The ZNRs deposited on solvothermally grown seed layer have random distribution and non-uniformity due to poor nucleation of ZNRs. So it can be analyzed that solvothermally grown seed layer has a large particle size compared to the particle size of the other three samples. ZNRs deposited on the ZnO QDs seed layer are well decorated, better vertically aligned, and high packing density throughout the surface. The height and thickness are also consistent in ZnO QDs seed layer based ZNRs. It is possible due to good crystalline and uniform particle size (which is also supported by TEM image in

the inset of Figure 4.4 (c)) of ZnO QDs seed layer.

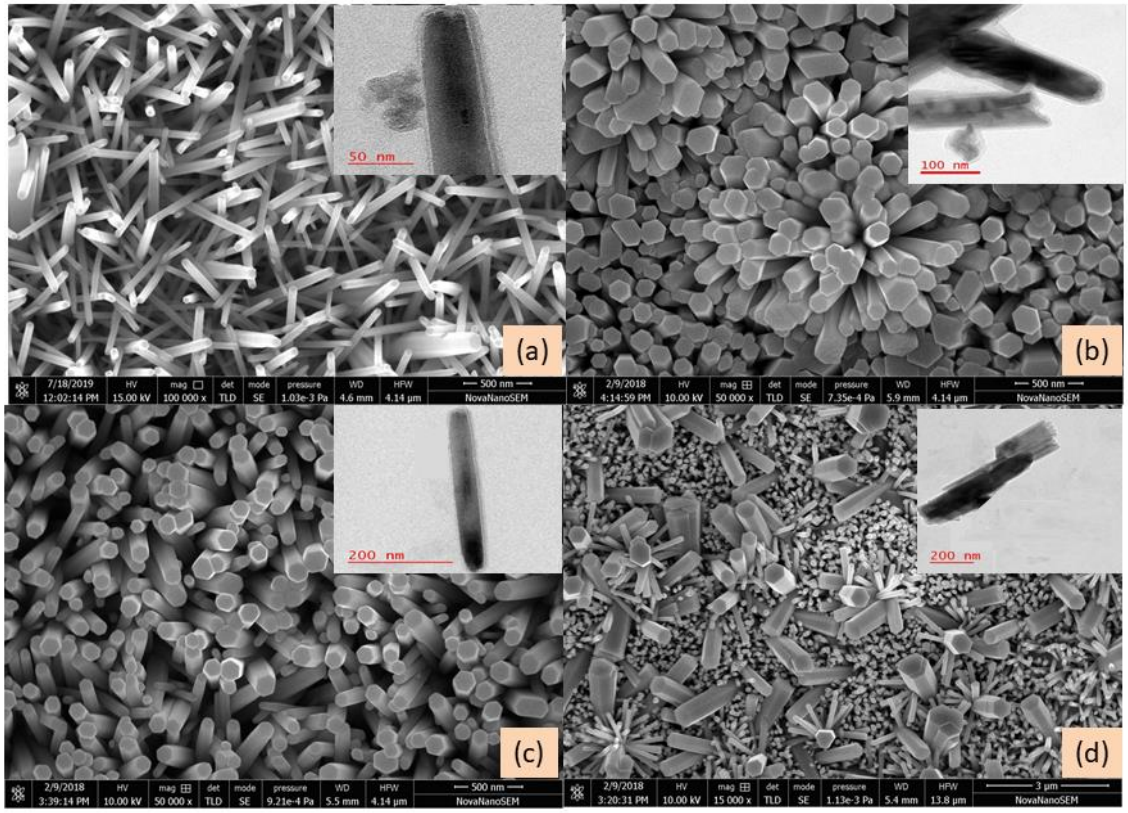

Figure 4.4: Top view of ZnO nanorods grown on different seed layers of (a) drop-cast (b) spin coated (ZnO NPs) (c) spin coated (ZnO QD) (d) solvothermal.

Figure 4.5 shows the X-ray diffraction (XRD) pattern of ZNRs grown on four different seed layer samples (Drop-cast, NPs, QDs, and solvothermal). The XRD image shows that most of the dominant diffraction peaks are corresponds to the wurtzite phase of ZnO and reveals uniform crystallinity. The major high-intensity peaks, such as 002, 101, 103, and 111, are common in all four samples (JCPDS 65-3431). The indexed peaks at 2Θ≈31.77˚, 34.42˚, 36.25˚, 47.53˚, 56.60˚, 62.85˚, 66.38˚, 67.95˚ and 72.56˚ correspond to the reflections from (100), (002), (101), (102), (110), (103), (200), (112) and (004) crystal planes of the wurtzite phase ZnO, whereas others peaks belong to the crystal plane of FTO. The intense and strongest peak was observed for the (002) plane. It is analyzed from the XRD pattern that the extra peak in the QDs based ZNRs sample

is coming at 2θ=56.60° and 72.56° due to the good orientation of ZNRs along the c-axis. So, it can be concluded from the XRD pattern that the QDs based ZNRs have a uniform and better crystallinity compared to other samples.

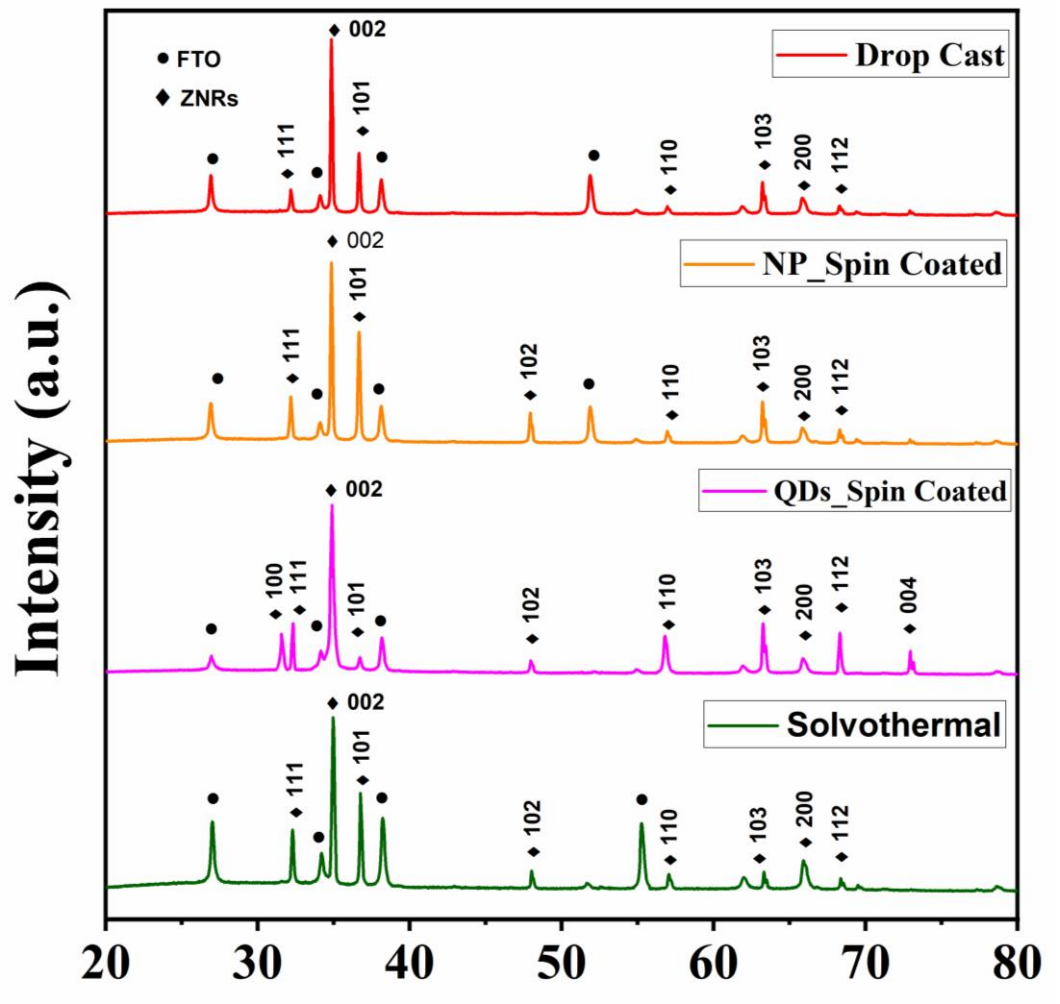

Figure 4.5: XRD pattern of ZnO NR grows on different ZnO seed layers deposited using (a) drop-cast (b) spin coated (ZnO NPs) (c) spin coated (ZnO QD) (d) solvothermal.

4.3.2 Optical Characterization

The optical absorbance and photoluminescence (PL) in the four types of seed layers on FTO coated substrate are plotted in Figure 4.6. A sharp change in absorbance has been observed at 395 nm wavelength in three seed layers (Drop-cast, NPs, and solvothermal based samples), while the QDs based seed layer sample has absorbance change at a wavelength of 375 nm. The optical characteristics are also verified by

photoluminance (PL) emission spectra, where the intensity curve of PL is matched with the band edge of absorbance spectra. The QDs deposited seed layer sample has lower band edge spectra, which is due to the smaller particle size with respect to the other three samples. It can be observed from Figure 4.6 that nanoparticle and drop-cast seed layer based samples have similar absorbance pattern, which is also confirmed from the PL emission graph. The optical band gap is also calculated by using the Tauc plot corresponding to the respective graph depicted in Figure 4.7.

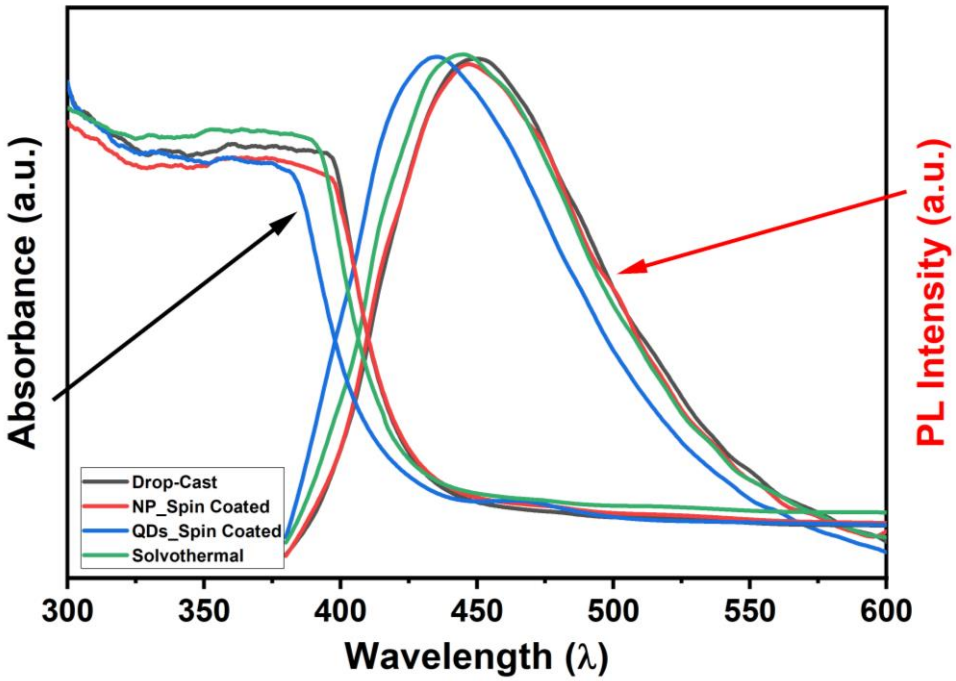

Figure 4.6: Photoluminescence emission and optical absorbance spectra of ZnO seed layer samples deposited on FTO substrate.

An abrupt change in absorbance spectra near the optical bandgap edge of ZNRs is calculated by the Tauc relationship [163]. The Tauc relationship is given as:

$$\alpha h\upsilon = A(h\upsilon - E_g)^m$$

Where $\alpha = 2.33 \log (T/d)$ is the absorbance coefficient, d is the film thickness, and $h\nu = 1240/[\text{incident light (nm)}]$ is the photon energy. The absorption in ZNRs can be written

as A = log (1/T). The estimated bandgap is 2.95 eV for drop-cast, 3 eV for NP, 3.05 eV for solvothermal, and ~3.1 eV for QDs based seed layer sample, which have been derived from the plot of $(\alpha h\nu)^{1/2}$ versus ($h\nu$). The derived optical band gap value can be correlated to the particle size of seed layer samples. The larger optical band gap of ZnO QDs seed layer based ZNRs sample calculated from the Tauc plot confirms the smaller particle size compared to other samples.

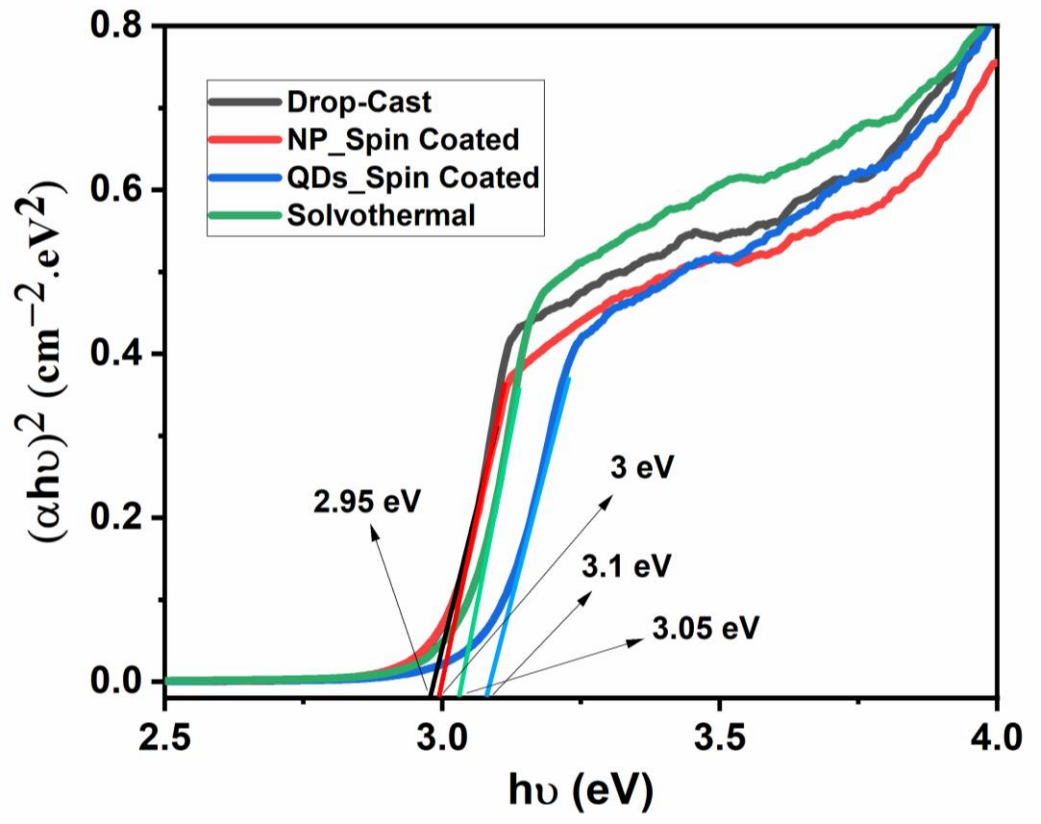

Figure 4.7: Tau plots for different ZnO seed layer samples.

The transmittance spectra of ZNRs grown on different ZnO seed layer is recorded by UV-Vis spectrometer for the wavelength range from 250 nm to 800 nm, as shown in Figure 4.8. The ZNRs grown on the ZnO QDs seed layer exhibits enhanced transmittance spectra in the visible range (from 400 nm to 700 nm) because of vertically oriented ZNRs compared to the other three samples. The ZNRs grown on nanoparticle and drop-cast based seed layer substrate have almost similar transmittance spectra but

less than the transmittance spectra of ZnO QDs seed layer based ZNRs. The reduction in transmittance spectra in ZnO nanoparticle and drop-cast based sample is because of photon scattering phenomena, while the ZNRs deposited on solvothermally grown seed layer based sample have reduced transmittance due to random growth of ZNRs and an increase in surface roughness of the samples. Note that the optical band gap for ZNRs can also be derived from the transmittance spectrum. The ZNRs have strong band edge transmittance near ~370 nm due to crystalline ZNRs, which reveal more transmittance towards the visible range. In addition, ZNRs deposited on ZnO QDs seed layer having more transmittance among all samples due to single crystallinity, uniform distribution, and vertically well-aligned on the substrate or in other words, solvothermal seed layer based sample has less transmittance due to more scattering within ZNRs. The less transmittance in solvothermal-based ZNRs sample results in less optical absorbance for PSC D, consequently poor device performance.

4.3.3 Electrical Characterization

The four perovskite solar cells' impedance measurement is recorded at an applied voltage of 1 V in the frequency range of 1 kHz–1 MHz, as shown in Figure 4.9. It is estimated from Figure 4.9 that the impedance is lowest for PSC C because of fewer defects in the electron transport layer. The current density-voltage (J-V) characteristics of the solar cells in the PTAA/$CH_3NH_3PbI_3$/ZNRs structure on the different types of seed layer are shown in Figure 4.10. The J-V characteristics reveal that power conversion efficiency is maximum for PSC C, which has a seed layer of quantum dots. It is also observed that there is no significant change in PCE of drop-cast and NP seed layer based PSCs. The FF of PSC C is highest while it is lowest in the case of PSC D. The possible reason for that is ZNRs of PSC C are well aligned and perpendicular to the

substrate, so that collection of charges takes place effectively. The FF is decreased due to the fact that the NR is not well aligned and not perpendicular to the c-axis in PSC A and D. The V_{OC} is minimum in case of solvothermal deposited PSC due to more internal series resistance and more chance of short-circuiting of the device. Whereas V_{OC} is maximum in the case of QDs seed layer based PSC due to lower series resistance. The increment in the V_{OC} is observed due to better alignment of ZNRs (As shown in SEM image) or less chance of short-circuiting and long electron pathway in the QDs seed layer based PSC. The photovoltaic parameters of four types of cells based on different seed layers are compared in Table 4.1.

Table 4.1: Photovoltaic parameter of different PSCs based on different seed layers**.**

ZnO Seed Layer	**V_{OC}**	**J_{SC}**	**FF**	**Efficiency (%)**
PSC A	0.95	19.26	0.58	9.12
PSC B	0.98	17.77	0.55	9.68
PSC C	1.01	19.14	0.64	10.69
PSC D	0.91	13.98	0.48	6.09

The overall optical absorbance is higher in both devices (PSC A and C) due to the large surface to volume ratio, which results in more current density. The voids and defects in the solvothermally deposited seed layer-based device enhance the possibility of recombination of electron-holes, resulting in a decrease in PSCs' performance. The distribution of ZNRs is non-uniform, so more voids and defect states in ZNRs, which results in a decrement in the V_{OC} as well as current-density in PSC D.

External quantum efficiency (EQE) of the solar cell is determined by using the following relation [164]:

$$EQE = 1240 \times \left(\frac{R}{\lambda}\right) \times 100\% \tag{4.5}$$

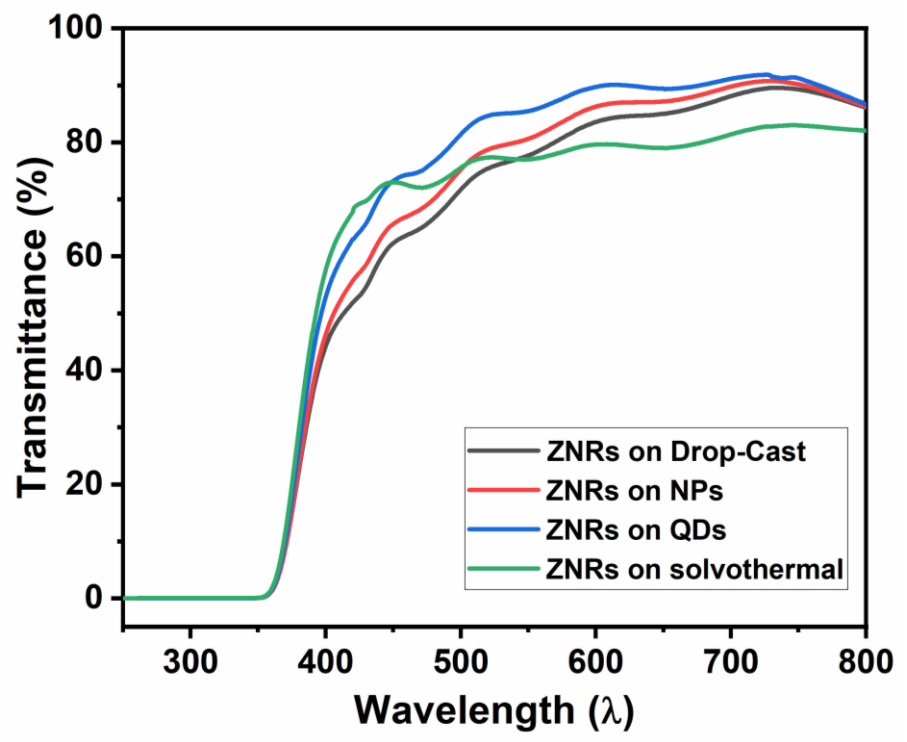

Figure 4.8: Transmittance spectra of ZnO nanorods deposited on various ZnO seed layer

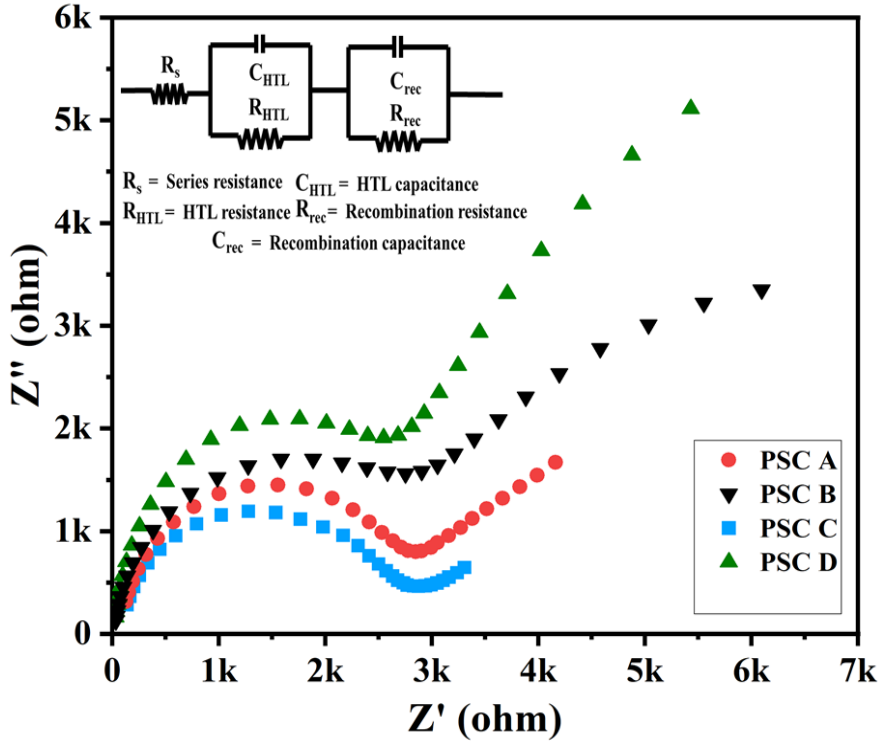

Figure 4.9: Impedance characteristics of PSCs A, B, C, & D

where "R" is the photoresponsivity and λ is the wavelength of the incident light. EQE for all the PSCs has been plotted in Figure 4.11 to compare the optical energy to electrical energy conversion in the selected wavelength range. The measured EQE is almost identical (~75%) for PSC A and PSC B in the range of 300-900 nm.

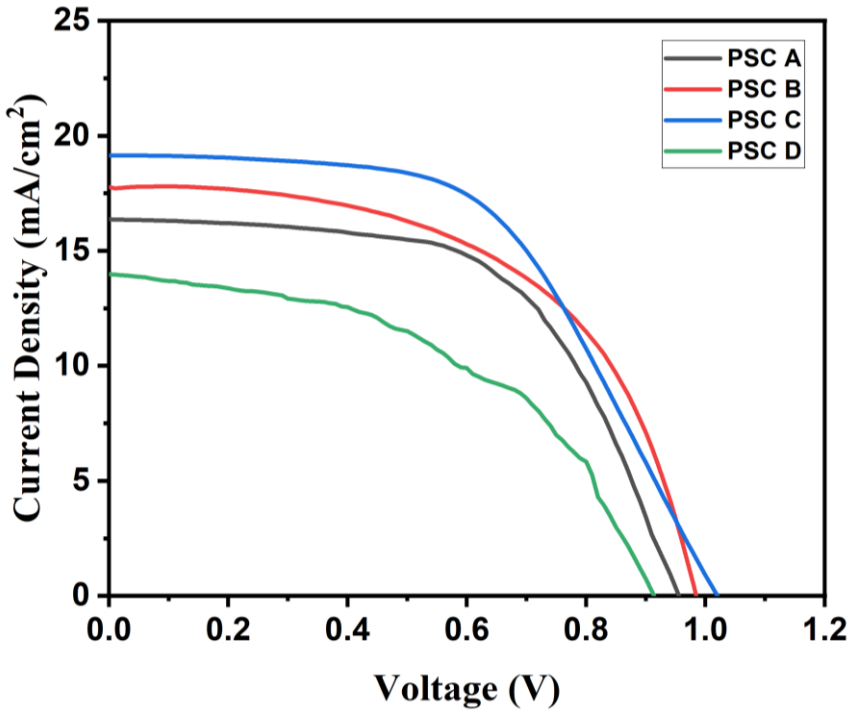

Figure 4.10: Current density vs voltage (J-V) curve of four ZNRs based PSCs fabricated on different ZnO seed layers

The highest EQE is obtained in PSC C, which again confirms its superior performance over the other three devices. Photon corresponding to this wavelength is well absorbed in the PSC C, and the generated charge carriers are transported effectively to the electrode. However, a significant improvement in the EQE of PSC B is also observed due to the growth of less defective ZNRs in a particular direction, which enhances the considerable absorption of light and also helps in collecting the generated charge carriers.

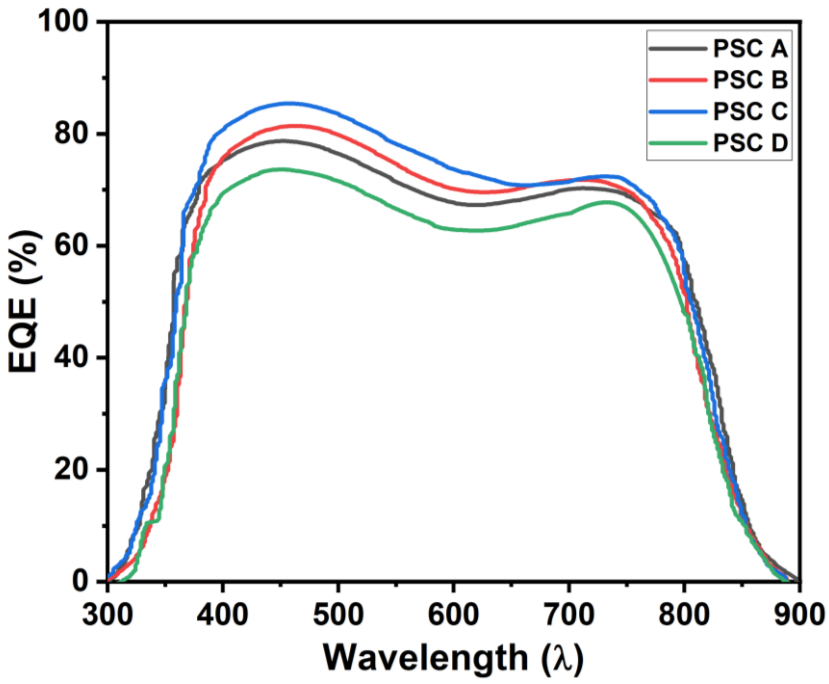

Figure 4.11: External quantum efficiency (EQE) of PSCs A, B, C, and D

4.4 Conclusion

The different types of seed layers based PSCs are fabricated and characterized for the performance improvement in the present chapter. The FTO/seed layer/ ZNRs/$CH_3NH_3PbI_3$/PTAA/Au structure is implemented on the glass substrate. The identical growth technique is used for the ZNRs in four types of seed layer based PSCs. The comparative study shows that the ZNRs grown on the ZnO QDs seed layer is more suitable for the perovskite-based solar cells. The current density (J_{SC}) of 19.14 mA/cm^2, V_{OC} of 1.01, fill factor of 0.64, and PCE of 10.69% have been achieved for ZnO QDs seed layer based PSC. The improvement in the solar parameters is attributed to the well align ZNRs grown on the seed layer with smaller particle size (ZnO QDs), directly affecting the V_{OC} and FF of the PSC. ZnO QDs based seed layer on the FTO substrate is uniform and more compact, which provides better nucleation sites for the vertically aligned ZNRs with a high surface to volume ratio.